
Gradient-based Editing of Memory Examples for Online Task-free Continual Learning

Xisen Jin Arka Sadhu Junyi Du Xiang Ren
University of Southern California
{xisenjin, asadhu, junyidu, xiangren@usc.edu}

Abstract

We explore task-free continual learning (CL), in which a model is trained to avoid catastrophic forgetting in the absence of explicit task boundaries or identities. Among many efforts on task-free CL, a notable family of approaches are memory-based that store and replay a subset of training examples. However, the utility of stored seen examples may diminish over time since CL models are continually updated. Here, we propose Gradient based Memory EDiting (GMED), a framework for editing stored examples in continuous input space via gradient updates, in order to create more “challenging” examples for replay. GMED-edited examples remain similar to their unedited forms, but can yield increased loss in the upcoming model updates, thereby making the future replays more effective in overcoming catastrophic forgetting. By construction, GMED can be seamlessly applied in conjunction with other memory-based CL algorithms to bring further improvement. Experiments validate the effectiveness of GMED, and our best method significantly outperforms baselines and previous state-of-the-art on five out of six datasets¹.

1 Introduction

Learning from a continuous stream of data – referred to as *continual learning (CL)* or *lifelong learning* – has recently seen a surge in interest, and many works have proposed ways to mitigate CL models’ catastrophic forgetting of previously learned knowledge [20, 32, 33]. Here, we study online *task-free* CL [3], where task identifiers and boundaries are absent from the data stream. This setting reflects many real-world data streams [6, 25] and offers a challenging testbed for online CL research.

Memory-based methods, a prominent class of approaches used for task-free continual learning, store a small number of training examples (from the data stream) in a memory and replay them at the later training iterations [33, 34]. Existing methods operate over the original examples in the data-stream and focus on identifying samples to populate the memory [4, 9] and finding samples in the memory to be replayed [2]. However, for continually updating models, using stored-seen examples in their original form, may lead to diminishing utility over time — i.e., model may gradually memorize the stored examples after runs of replay, as the memory refreshes slowly. An alternate approach is to use generative models to create samples that suffers more from forgetting such as in GEN-MIR in [2]. In practice, training the generator network with limited data is challenging and leads to low-quality generated examples. Further, in the online learning setup, the generative model itself suffers from forgetting. As such, generative models perform worse than their memory counter-parts.

In this paper, we present a novel memory-based CL framework, Gradient based Memory EDiting (**GMED**), which looks to directly “edit” (via a small gradient update) examples stored in the replay memory. These edited examples are stored (replacing their unedited counterparts), replayed, and further edited, thereby making the future replays more effective in overcoming catastrophic forgetting.

¹Code can be found at <https://github.com/INK-USC/GMED>.

Since no explicit generative model is involved, GMED approach retains the advantages of memory-based methods and is straightforward to train only inducing a small computation overhead.

The main consideration in allowing “editing” via a gradient update is the choice of the optimization objective. In light of recent work on designing alternative replay strategies [2, 7, 40], we hypothesize that “interfering” examples (*i.e.*, past examples that suffer from increased loss) should be prioritized for replay. For a particular stored example, GMED finds a small update over the example (“edit”) such that the resulting edited example yields the most increase in loss when replayed. GMED additionally penalizes the loss increase in the edited example to enforce the proximity of the edited example to the original sample, so that the edited examples stay in-distribution. As a result, replaying these edited examples is more effective in overcoming catastrophic forgetting. Since GMED focuses only on editing the stored examples, by construction, GMED is modular, *i.e.*, it can be seamlessly integrated with other state-of-the-art memory-based replay methods [2, 5, 26].

We demonstrate the effectiveness of GMED with a comprehensive set of experiments over six benchmark datasets. In general, combining GMED with existing memory-based approaches results in consistent and statistically significant improvements with our single best method establishing a new state-of-art performance on five datasets. Our ablative investigations reveal that the gains realized by GMED are significantly larger than those obtained from regularization effects in random perturbation, and can be accumulated upon data augmentation to further improve performance.

To summarize, our contributions are two-fold: (i) we introduce GMED, a modular framework for task-free online continual learning, to edit stored examples and make them more effective in alleviating catastrophic forgetting (ii) we perform intensive set of experiments to test the performance of GMED under various datasets, parameter setups (*e.g.*, memory size) and competing baseline objectives.

2 Related Work

Continual Learning studies the problem of learning from a data stream with changing data distributions over time [20, 23]. A major bottleneck towards this goal is the phenomenon of catastrophic forgetting [33] where the model “forgets” knowledge learned from past examples when exposed to new ones. To mitigate this effect, a wide variety of approaches have been investigated such as adding regularization [1, 19, 30, 43], separating parameters for previous and new data [24, 36, 37], replaying examples from memory or a generative model [26, 33, 38], meta-learning [18]. In this work, we build on memory-based approaches which have been more successful in the online task-free continual learning setting that we study.

Online Task-free Continual Learning [3] is a specific formulation of the continual learning where the task boundaries and identities are not available to the model. Due to its broader applicability to real-world data-streams, a number of algorithms have been adapted to the task-free setup [2, 14, 15, 22, 44]. In particular, memory-based CL algorithms which store a subset of examples and later replay them during training, have seen elevated success in the task-free setting. Improvements in this space have focused on: *storing diverse examples* as in Gradient-based Sample Selection (GSS) [4], and *replaying examples with larger estimated “interference”* as in Maximally Interfered Retrieval (MIR) with experience replay [2]. In contrast, GMED is used in conjunction with memory-based approaches and explicitly searches for an edited example which is optimized to be more “effective” for replay.

Replay Example Construction. Moving away from replaying real examples, a line of works on *deep generative replay* [17, 35, 38] generates synthetic examples to replay with a generative model trained online. GEN-MIR [2] is further trained to generate examples that would suffer more from interference for replay. However, training a generative network is challenging, even more so in the online continual learning setup where the streaming examples are encountered only once leading to poorly generated examples. Moreover, the forgetting of generative networks themselves cannot be perfectly mitigated. As a result, these methods generally perform worse than their memory-based counter-parts. Instead of generating a new example via a generator network, GMED uses gradient updates to directly edit the stored example thereby retaining advantages of memory-based techniques while creating new samples.

Novel examples can also be constructed via *data augmentation* (*e.g.* random crop, horizontal flip) to help reduce over-fitting over the small replay memory [5]. Unlike GMED, these data-augmentations are usually pre-defined and cannot adapt to the learning pattern of the model. Constructing edited examples has also been used for adversarial robustness [31, 39]. The key difference lies in the

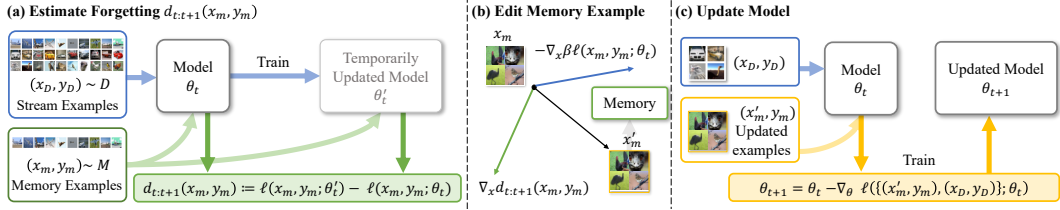


Figure 1: **A schematic of GMED framework.** (a) Given an example from the data-stream (x_D, y_D) at time t , the model randomly draws an example from the memory (x_m, y_m) and estimates “interference” after one-step roll-out (Eq. 2). (b) The example drawn from the memory is then updated using our proposed editing objective (Eq. 3) via gradient ascent, resulting in (\hat{x}_m, y_m) , and written back into the memory. (c) Finally, the model is updated using the edited example (\hat{x}_m, y_m) and the example from the data-stream (x_D, y_D) (Eq. 4).

optimization objective: while adversarial construction focuses on finding mis-classified examples [13, 28], GMED aims at constructing “interfered” examples that would suffer from loss increase in future training steps.

3 Method

We introduce the formulation of online task-free continual learning (Sec. 3.1) and then present our gradient-based memory editing method GMED (Sec. 3.2) and detail how GMED can be integrated with experience replay (Sec. 3.3) and other memory-based CL algorithms (Sec. 3.4).

3.1 Problem Formulation

In continual learning (CL), we consider a (potentially infinite) stream D of labeled examples (x, y) , having a non-stationary data distribution – *i.e.*, the data distribution $p(x, y)$ evolves over time. Let (x_t, y_t) denote the labeled example (or a mini-batch of examples) received by the model at time-step t in the data-stream D . We assume, for simplicity, that (x_t, y_t) is generated by first sampling a latent “task” $z \sim p(z; t)$, followed by sampling a data example from a conditional data distribution $p(x, y|z)$, – *i.e.*, $(x_t, y_t) \sim p(x, y|z)$. Here $p(z; t)$ is non-i.i.d and time-dependent. In *task-free* CL setting, the latent task z is *not* revealed to the model. Finally, we emphasize that while models in task-aware setup proceed to the next task only after convergence on the current task [19, 43], this work focuses on **online task-free CL** setup [8, 9]. It simulates a practical setting where models must perform online update on every incoming example, without accumulating examples within a task.

Following above definitions, our goal is to learn a classification model $f(x; \theta)$ on the data stream D that can preserve its performance over all the tasks in D . At time step t during the training process, the model is updated to minimize a predefined empirical loss $\ell(x_t, y_t; \theta)$ on the newly received example (x_t, y_t) , without increasing the loss on the previously visited examples (before t). Specifically, let $p_c(x, y; T)$ denotes the distribution of the examples visited until the time step T . We look to minimize the expected loss $\mathbb{E}_{p_c(x, y; T)} \ell(x, y; \theta)$ – *i.e.*, retaining performance on tasks encountered before T .

3.2 Gradient based Memory Editing (GMED)

In online task-free continual learning, examples visited earlier cannot be accessed (revisited) and thus computing the loss over all the visited examples (in D) is not possible. To deal with this challenge, memory-based CL algorithms store and (continuously) maintain a set of visited examples in a fixed-size memory and use them for replay or regularization in the future training steps [26, 33]. For instance, in Experience Replay (ER) [33] the examples are randomly sampled from the memory for replay; whereas recent works explore more sophisticated replay strategies, such as Maximally Interfered Retrieval with experience replay (ER-MIR) [2] where memory examples which interfere the most with the newly visited example are selected for replay. However, these algorithms only train over samples drawn from a small replay memory in their original form. As such, the utility of the stored examples could diminish over time as the model could potentially memorize these examples if the memory examples are refreshed in a slow pace – which is found often the case [5].

We address the above limitation in our proposed approach Gradient based Memory Editing (GMED) by allowing examples stored in the memory to be edited in the continuous input space, illustrated in Figure 1. The editing step is guided by an optimization objective instead of being pre-defined and involves drawing examples from the memory, editing the drawn examples, replaying the edited

examples and at the same time writing the edited examples back to the memory. We now state our optimization objectives of example editing followed by algorithmic details of GMED.

Editing Objective. Clearly, the most crucial step involved in GMED is identifying “how” should the stored examples in the memory be edited to reduce catastrophic forgetting of early examples. If (x_m, y_m) denotes an example drawn from the memory M , the goal is to design a suitable editing function ϕ to generate the edited example \hat{x}_m where $\hat{x}_m = \phi(x_m)$. Such “editing” process can also be found in white-box adversarial example construction for robustness literature [13] where the task is to find an “adversarial” example (x', y) that is close to an original example (x, y) but is mis-classified by the model. Typically, adversarial example construction utilizes the gradients obtained from the classifier and edits the examples to move towards a different target class. While, in the context of continual learning, the editing objective should be different. We employ a similar hypothesis as previous works [2, 7, 40] that examples that are likely forgotten by models should be prioritized for replay. Accordingly, we edit examples so that they are more likely to be forgotten in future updates. With this objective of editing in place, we detail the process of incorporating GMED with Experience Replay (ER).

3.3 The GMED Algorithm with ER

Algorithm 1 summarizes the process and Figure 1 provides a schematic of the steps involved in GMED. At time step t , the model receives a mini-batch of the stream examples (x_D, y_D) from the training stream D , and randomly draws a same number of memory examples (x_m^k, y_m) from the memory M , which we assume has already been drawn for replay for k times. We first compute the “interference” (*i.e.*, loss increase) on the memory example (x_m^k, y_m) when the model performs one gradient update on parameters with the stream example (x_D, y_D) .

$$\theta'_t = \theta_t - \nabla_{\theta} \ell(x_D, y_D; \theta_t); \quad (1)$$

$$d_{t:t+1}(x_m^k, y_m) = \ell(x_m^k, y_m; \theta'_t) - \ell(x_m^k, y_m; \theta_t), \quad (2)$$

where θ_t and θ'_t are model parameters before and after the gradient update respectively. Then, we perform a step of gradient update on (x_m^k, y_m^k) by maximizing its “loss increase” in the next one step of training, while using a regularization term $\ell(x_m, y_m; \theta_t)$ to penalize the loss increase evaluated with the current model checkpoint. The iterative update is written as,

$$x_m^{k+1} \leftarrow x_m^k + \gamma^k \alpha \nabla_x [d_{t:t+1}(x_m^k, y_m) - \beta \ell(x_m^k, y_m; \theta_t)], \quad (3)$$

where the hyper-parameter α controls the overall stride of the edit and is tuned with first three tasks together with the regularization strength β . γ is a decay factor of edit performed on the model. A decay factor γ less than 1.0 could effectively prevent x_m^k from drastically deviating from their original state, while $\gamma = 1.0$ indicates no decay. We note that we cannot perform constrained edits that strictly adhere to a distance budget w.r.t original examples, as it requires storing original examples which introduces extra memory overhead.

Following Eq. 3, we perform a gradient update on x to increase its “interference”. The algorithm then discards θ'_t , and updates model parameters θ_t using the edited memory example (x_m^{k+1}, y_m) and the stream example (x_D, y_D) , in a similar way to ER.

$$\theta_{t+1} = \theta_t - \nabla_{\theta} \ell(\{(x_m^{k+1}, y_m), (x_D, y_D)\}; \theta_t). \quad (4)$$

We replace the original examples in the memory with the edited example. In this way, we continuously edit examples stored in the memory alongside training.

Algorithm 1: Gradient Memory EDiting with ER (ER+GMED)

- 1: **Input:** learning rate τ , edit stride α , regularization strength β , decay rate γ , model parameters θ
- 2: **Receives:** stream example (x_D, y_D)
- 3: **Initialize:** replay memory M
- 4: **for** $t = 1$ **to** T **do**
- 5: //when $\gamma = 1$, k is not required
- 6: $(x_m, y_m) \sim M$; $k \leftarrow \text{replayed_time}(x_m, y_m)$
- 7: $\ell_{\text{before}} \leftarrow \text{loss}(x_m, y_m, \theta_t)$;
- 8: $\ell_{\text{stream}} \leftarrow \text{loss}(x_D, y_D, \theta_t)$
- 9: //update model with stream examples
- 10: $\theta'_t \leftarrow \text{SGD}(\ell_{\text{stream}}, \theta_t, \tau)$
- 11: //evaluate forgetting of memory examples
- 12: $\ell_{\text{after}} \leftarrow \text{loss}(x_m, y_m, \theta'_t)$
- 13: $d \leftarrow \ell_{\text{after}} - \ell_{\text{before}}$
- 14: //edit memory examples
- 15: $x'_m \leftarrow x_m + \gamma^k \alpha \nabla_x (d - \beta \ell_{\text{before}})$
- 16: $\ell = \text{loss}(\{(x'_m, y_m), (x_D, y_D)\}, \theta_t)$
- 17: $\theta_{t+1} \leftarrow \text{SGD}(\ell, \theta_t, \tau)$
- 18: replace (x_m, y_m) with (x'_m, y_m) in M
- 19: reservoir_update(x_D, y_D, M)
- 20: **end for**

3.4 Applying GMED with Data Augmentation, MIR and GEM

Since the process to edit the original examples in GMED is modular, we can integrate GMED with a range of existing memory-based CL algorithms. In addition to ER, we also explore ER with data augmentation (ER_{aug}) [5], ER-MIR [2] and GEM [26] in our experiments.

ER_{aug} applies standard data augmentations (*e.g.*, random cropping, horizontal flipping, denoted as \mathcal{T}) to examples (x_m, y_m) drawn from the memory which are replayed at each time step. In ER_{aug}+GMED, we edit original example x_m and replay both the augmented example $\mathcal{T}(x_m)$ and the edited example \hat{x}_m . To keep the number of replayed examples the same, for ER_{aug} method, we also replay both the edited example $\mathcal{T}(x_m)$ and the original example x_m . Finally, we write the edited example \hat{x}_m to the memory.

For integration with ER-MIR (denoted henceforth as MIR for brevity), recall that MIR retrieves and then replays the most “interfering” examples in the memory at each time-step. Thus, making GMED edits on the MIR-retrieved examples may induce a loop of further increasing “interference” of the examples that are already the most “interfering” ones. Instead, in our MIR+GMED implementation, we edit a mini-batch of examples randomly sampled from the memory — a process that is *independent* of the MIR replay operation². This random sampling may help prevent GMED editing from intensifying potential biases created from the MIR retrieval process (*e.g.*, retrieved examples are edited and thus become more interfered). Similarly, For GEM+GMED, we also apply GMED to edit a mini-batch of randomly sampled examples.

Details of the integrated algorithms (*i.e.*, ER_{aug}+GMED, MIR+GMED, and GEM+GMED) can be found in Algorithms 2, 3 and 4 in Appendix B. We leave more sophisticated integration of GMED to existing CL algorithms *e.g.* by optimizing the retrieval and editing operations jointly to future work.

4 Experiments

Our experiments address the following research questions: (i) what are the gains obtained by integrating GMED with existing memory-based CL algorithms and how these gains compare across datasets, methods and memory sizes? (ii) how useful are GMED edits in alleviating catastrophic forgetting, and what part of it can be attributed to the design of the editing objective function? (iii) what role do the various components and parameters in the GMED play and how they affect the performance. In the rest of this section, we first briefly describe the datasets (Sec. 4.1) and the compared baselines (Sec. 4.2). We then detail our main results comparing across memory-based algorithms (Sec. 4.3), validate the effectiveness of GMED-edits and the editing objective in mitigating catastrophic forgetting (Sec. 4.4), followed by ablative study over its components (Sec. 4.5).

4.1 Datasets

We use six public CL datasets in our experiments. **Split / Permuted / Rotated MNIST** are constructed from the MNIST [21] dataset which contains images of handwritten digits. Split MNIST [12] creates 5 disjoint subsets based on the class labels and considers each subset as a separate task. The goal then is to classify over all 10 digits when the training ends. Permuted MNIST [12] consists of 10 tasks, where for a particular task a random permutation in the pixel space is chosen and applied to all images within that task. The model then has to classify over the 10 digits without knowing which random permutation was applied. Rotated MNIST [26] rotates every sample in MNIST by a fixed angle between 0 to 180. Similar to the previous datasets, the goal is to classify over 10 digits without any knowledge of the angle of rotation. For all MNIST experiments, each task consists of 1,000 training examples following [2]. We also employ **Split CIFAR-10 and Split CIFAR-100**, which comprise of 5 and 20 disjoint subsets respectively based on their class labels. The model then classifies over the space of all class labels. Similarly, **Split mini-ImageNet** [2] splits the mini-ImageNet [10, 42] dataset into 20 disjoint subsets based on their labels. The models classify over all 100 classes.

Following the taxonomy of [41], the Split MNIST, Split CIFAR-10, Split CIFAR-100, and Split mini-ImageNet experiments are categorized under class-incremental setup, while Permuted and Rotated MNIST experiments belong to domain-incremental setup. We note that our results are not comparable

²This also ensures the integrated approach will replay the same number of examples as the baselines, yielding a fair comparison.

Table 1: Mean and standard deviation of final accuracy (%) for non-model-expansion-based approaches on 6 datasets. For Split mini-ImageNet and Split CIFAR-100 datasets, we set the memory size to 10,000 and 5,000 examples; we use 500 for other datasets. * and ** over GMED methods indicate significant improvement over the counterparts without GMED with p -values less than 0.1 and 0.05 respectively in single-tailed paired t-tests. We report results in 20 runs for GEM, ER, MIR, and ER_{aug} and their GMED-integrated versions, and 10 runs for others. † over “previous SOTA” results indicates that the best GMED method (**bolded** for each dataset) outperforms the previous SOTA with statistically significant improvement ($p < 0.1$).

Methods / Datasets	Split MNIST	Permuted MNIST	Rotated MNIST	Split CIFAR-10	Split CIFAR-100	Split mini-ImageNet
Fine tuning	18.80 ± 0.6	66.34 ± 2.6	41.24 ± 1.5	18.49 ± 0.2	3.06 ± 0.2	2.84 ± 0.4
AGEM [8]	29.02 ± 5.3	72.17 ± 1.5	50.77 ± 1.9	18.49 ± 0.6	2.40 ± 0.2	2.92 ± 0.3
GSS-Greedy [4]	84.16 ± 2.6	77.43 ± 1.4	73.66 ± 1.1	28.02 ± 1.3	19.53 ± 1.3	16.19 ± 0.7
BGD [44]	13.54 ± 5.1	19.38 ± 3.0	77.94 ± 0.9	18.23 ± 0.5	3.11 ± 0.2	24.71 ± 0.8
ER [33]	81.07 ± 2.5	78.65 ± 0.7	76.71 ± 1.6	33.30 ± 3.9	20.11 ± 1.2	25.92 ± 1.2
ER + GMED	82.67** ± 1.9	78.86 ± 0.7	77.09* ± 1.3	34.84** ± 2.2	20.93* ± 1.6	27.27** ± 1.8
MIR [2]	85.72 ± 1.2	79.13 ± 0.7	77.50 ± 1.6	34.42 ± 2.4	20.02 ± 1.7	25.21 ± 2.2
MIR + GMED	86.52** ± 1.4	79.25 ± 0.8	79.08** ± 0.8	36.17* ± 2.5	21.22** ± 1.0	26.50** ± 1.3
ER _{aug} [5]	80.14 ± 3.2	78.11 ± 0.7	80.04 ± 1.3	46.29 ± 2.7	18.32 ± 1.9	30.77 ± 2.2
ER _{aug} + GMED	82.21** ± 2.9	78.13 ± 0.6	80.61* ± 1.2	47.47* ± 3.2	19.60 ± 1.5	31.81* ± 1.3
Previous SOTA	85.72† ± 1.2	79.23 ± 0.7	80.04† ± 1.3	46.29† ± 2.7	20.02† ± 1.7	30.77† ± 2.2
iid online	85.99 ± 0.3	73.58 ± 1.5	81.30 ± 1.3	62.23 ± 1.5	18.13 ± 0.8	17.53 ± 1.6
iid offline (upper bound)	93.87 ± 0.5	87.40 ± 1.1	91.38 ± 0.7	76.36 ± 0.9	42.00 ± 0.9	37.46 ± 1.3

to works that employ a different setup over the same dataset (*e.g.*, results on domain-incremental Split CIFAR-100 are not comparable).

4.2 Compared Methods

We compare against several task-free memory based continual learning methods namely, Experience Replay (ER) [33], Averaged Gradient Episodic Memory (AGEM) [8], Gradient based Sample Selection (GSS) [4], and Maximally Interfering Retrieval (MIR) [2]. We omit the generative replay method GEN-MIR proposed together in [2] as it underperforms their memory-based counterparts even on simple datasets such as Split MNIST.

We also compare with data augmentation [5] such as random rotations, scaling, and horizontal flipping applied to memory examples drawn for replay in ER, noted as ER_{aug} (except for MNIST datasets). We also include regularization-based, model expansion-based and task-aware approaches, namely Bayesian Gradient Descent (BGD) [44], Neural Dirichlet Process Mixture Model (CN-DPM) [22], Progressive Networks (Prog.NN) [36], Compositional Lifelong Learning [29], Gradient Episodic Memory (GEM) [26] and Hindsight Anchor Learning (HAL) [7] respectively.

Finally, we report three baseline models: (i) Fine Tuning, where no continual learning algorithms are used for online updates to model parameters, (ii) iid Online, where we randomly shuffle the data stream, so that the model visits an i.i.d. stream of examples, and (iii) iid Offline, where multiple passes over the dataset is allowed. Appendix A provides more details on compared methods and their implementation details. We build our proposed GMED approach upon four baselines, noted as ER+GMED, MIR+GMED, GEM+GMED, and ER_{aug}+GMED.

Implementation Details. We set the size of replay memory as $10K$ for split CIFAR-100 and split mini-ImageNet, and 500 for all remaining datasets. Following [8], we tune the hyper-parameters α (editing stride) and β (regularization strength) with only the first three tasks. While γ (decay rate of the editing stride) is a hyper-parameter that may flexibly control the deviation of edited examples from their original states, we find $\gamma=1.0$ (*i.e.*, no decay) leads to better performance in our experiments. Results under different γ setups are provided in Appendix C, and in the remaining sections we assume no decay is applied. For model architectures, we mostly follow the setup of [2]: for the three MNIST datasets, we use a MLP classifier with 2 hidden layers with 400 hidden units each. For Split CIFAR-10, Split CIFAR-100 and Split mini-ImageNet datasets, we use a ResNet-18 classifier with three times less feature maps across all layers. See Appendix C for more details.

4.3 Performance Across Datasets

We summarize the results obtained by integrating GMED with different CL algorithms. In Table 1, we report the final accuracy and the standard deviation and make the following key observations.

Effectiveness of Memory Editing. As can be seen in Table 1, GMED significantly improves performance on 5 datasets when built upon ER and MIR respectively. The improvement of MIR+GMED

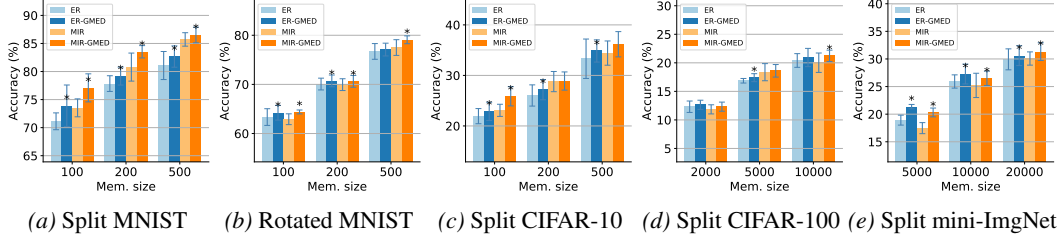


Figure 2: Performance of ER, GMED+ER, MIR, and GMED+MIR with different memory sizes. For mini-ImageNet dataset, we use memory sizes of 1K, 5K, 10K, and 20K examples; for Split CIFAR-100 dataset, we use 1K, 2K, 5K and 10K; for other datasets, we use 100, 200, 500, and 1000. * indicates whether the improvement of ER+GMED or MIR+GMED is significant with $p < 0.05$.

corroborates that the optimization in the continuous input spaces of GMED is complementary to sample selection over real examples as in MIR. We also notice significant improvement of ER_{aug} over GMED on 5 datasets. This indicates that the benefits induced by GMED go beyond regularization effects used to mitigate over-fitting.

Comparison across CL methods. From Table 1, we find MIR+GMED achieves the best performance on Split MNIST, Permuted MNIST, and Split CIFAR-100 datasets; while on Rotated MNIST, Split CIFAR-10 and Split mini-ImageNet dataset, ER_{aug} +GMED achieves the best performance. Performance of the best performing GMED method could significantly improve over previous SOTA on five datasets.

We further compare with a non-memory based CL approach, CN-DPM [22], which employs a generative model, a dynamically expanding classifier, and utilizes a short-term memory (STM). Following the setup in [16], we set the memory size for GMED so that two methods introduces the same amount of the overhead. Table 2 shows the results of ER, ER+GMED and the reported results of CN-DPM. Interestingly, ER by itself achieves comparable performance to model expansion approaches. ER+GMED further outperforms CN-DPM without any extra memory overhead compared to ER. Similarly, GMED outperforms *task-aware* model expansion approaches such as Prog. NN and the recently proposed compositional model expansion (CompCL) with a smaller memory overhead.

Performance under Various Memory Sizes. Figure 2 shows the performance of ER, ER+GMED, MIR, and MIR+GMED under various memory sizes. The improvement on Split MNIST and Split mini-ImageNet are significant with $p < 0.05$ over all memory size setups. On Rotated MNSIT and Split CIFAR-10 the improvements are also mostly significant. The improvement on Split CIFAR-100 is less competitive, probably because the dataset is overly difficult for class-incremental learning, from the accuracy around or less than 20% in all setups.

Performance on Data Streams with Fuzzy Task Boundaries. The experiments in Table 1

assume a clear task boundary. In Table 3, we report the result of using data-streams with fuzzy task boundaries on four datasets. We leave the complete results in Table 9 in Appendix. In this setup, the probability density of a new task grows linearly starting from the point where 50% of examples of

Table 2: Comparison with model-expansion-based approaches under the same memory overhead as CN-DPM. The overhead is the size of the replay memory plus the extra model components (e.g. a generator or modules to solve individual tasks), shown in the equivalent number of memory examples (#. Mem). † indicates quoted numbers are taken from the respective papers.

Method	Split MNIST		Split CIFAR-10		Split CIFAR-100	
	Acc.	#. Mem	Acc.	#. Mem	Acc.	#. Mem
CN-DPM†	93.23	2,581	45.21	6,024	20.10	21,295
Prog. NN	89.46	9,755	49.68	6,604	19.17	31,766
CompCL	91.27	9,755	45.62	6,604	20.51	31,766
ER	92.67	2,581	62.96	6,024	21.79	21,295
ER+GMED	94.16	2,581	63.28	6,024	22.12	21,295

Table 3: Performance of methods over data streams with fuzzy task boundaries. In this setup, examples from the next tasks are introduced and gradually dominate the stream when half of the examples from the current task is visited. * indicates whether the improvement is significant ($p < 0.05$)

Methods / Datasets	Split MNIST	Split CIFAR-10	Split mini-ImageNet
Vanilla	21.53 ± 0.1	20.69 ± 2.4	3.05 ± 0.6
ER	79.74 ± 4.0	37.15 ± 1.6	26.47 ± 2.3
MIR	84.80 ± 1.9	38.70 ± 1.7	25.83 ± 1.5
ER_{aug}	81.30 ± 2.0	47.97 ± 3.5	30.75 ± 1.0
ER + GMED	82.73* ± 2.6	40.57* ± 1.7	28.20* ± 0.6
MIR + GMED	86.17 ± 1.7	41.22* ± 1.1	26.86* ± 0.7
ER_{aug} + GMED	82.39* ± 3.7	51.38* ± 2.2	31.83 ± 0.8

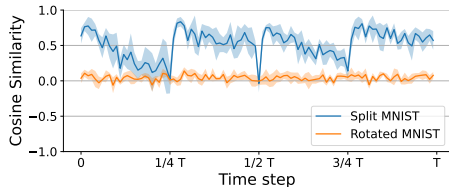


Figure 3: Cosine similarity between the optimal editing direction and direction from ER+GMED over training. The averaged similarity is 0.523 ± 0.014 and 0.035 ± 0.009 .

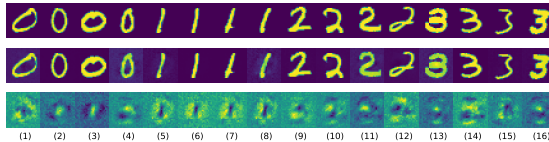


Figure 4: Visualization of the edited examples in Split MNIST in the ER-GMED approach. The first two rows show examples before and after editing, and the third row shows the differences.

the current task are visited. In particular, GMED improves performance in three datasets across ER, MIR and ER_{aug}.

Effectiveness of GMED in Task-Aware Setting. We additionally compare performance of other task-aware approaches (HAL, GEM, GEM+GMED) in Appendix H.

4.4 Ablation to Study the Effect of Memory-Editing

We present a set of experiments to validate that the gains obtained through the memory-editing step of GMED are indeed helpful towards alleviating catastrophic forgetting. Further, we show that these gains are distinct from those obtained through random perturbations or simple regularization effects.

Comparison to Optimal Editing Direction. At a particular time-step t , GMED identifies the edit direction using the stream example (x_D, y_D) and the memory sample (x_m, y_m) . To validate whether the edits proposed by GMED are indeed helpful, we compare GMED-edit to an ‘‘Optimal Edit’’ that minimizes the loss increase (‘‘interference’’) of all early training examples in one future time step.

To compute this Optimal Edit, we note that the total loss increase over all previously encountered examples would be $d_{t:t+1}^{1:t} = \sum_{i=1}^t d_{t:t+1}(x_i, y_i) = \sum_{i=1}^t [\ell(x_i, y_i; \theta_{t+1}) - \ell(x_i, y_i; \theta_t)]$, where $\theta_{t+1} = \theta_t - \nabla_{\theta} \ell(x_m, y_m; \theta_t) - \nabla_{\theta} \ell(x_D, y_D; \theta_t)$ is the model parameters after the training update on (x_D, y_D) and (x_m, y_m) . The Optimal Edit direction for the memory example x_m would be the gradient of $d_{t:t+1}^{1:t}$ w.r.t. x_m . Computing such optimal edits requires access to early training examples and is not practical in an online continual learning setup; we present it only for ablative purposes.

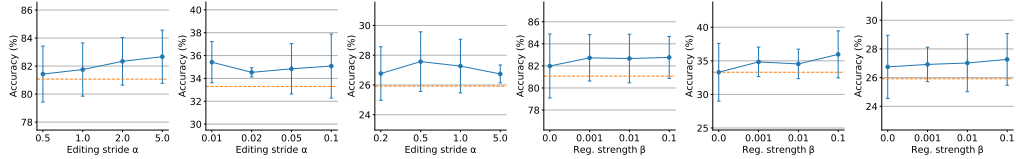
Figure 3 shows the cosine similarity of update directions (*i.e.*, the gradient of x_m) between GMED and the optimal editing strategy over Split MNIST and Rotated MNIST datasets. The averaged similarity over time is 0.523 ± 0.014 , 0.035 ± 0.009 on two datasets, averaged across 10 runs. Recall that random editing has an expectation of zero similarity. On Split MNIST dataset, where the improvement is the most significant, we notice a high similarity between the update directions of GMED and optimal editing. On Rotated MNIST where the improvement is less significant, the similarity is still positive on average but is lower than Split MNIST. It implies GMED-edits are generally consistent with explicitly reducing forgetting, but there is still space to improve. The results also imply the whether the edits of GMED aligns with editing is highly dependent on certain properties of datasets. We further include the classification performance of optimal editing in Appendix L.

Comparison with alternative Editing Objectives. While GMED objective editing correlates with that of Optimal Edit, we further validate the choice of the objective function and consider two alternatives to the proposed editing objective (Eq. 3): (i) Random Edit: memory examples are updated in a random direction with a fixed stride; (ii) Adversarial Edit: following the literature of adversarial example construction [13], the edit increases the loss of memory by following the gradient $\text{sgn} \nabla_x \ell(x_m, y_m; \theta)$. We report the comparison in Table 4.

We notice ER+Random Edit outperforms ER on split mini-ImageNet, which indicates adding random noise to memory examples helps in regularization. Even so, GMED-edits are as good or

Table 4: Alternative memory editing objectives or simply increasing the number of replayed examples. Comparison of Random Edit, Adversarial Edit (Adv. Edit) to our proposed objective in GMED. * indicates significant improvement ($p < 0.05$) compared to adversarial edit.

Methods / Datasets	Rotated MNIST	Split CIFAR-10	Split mini-ImageNet
ER	76.71 \pm 1.6	33.30 \pm 3.9	25.92 \pm 1.2
ER + Random Edit	76.42 \pm 1.3	32.26 \pm 1.9	26.50 \pm 1.3
ER + Adv. Edit	76.13 \pm 1.5	31.69 \pm 0.8	26.09 \pm 1.6
ER + GMED	77.50 \pm 1.6	34.84* \pm 2.2	27.27* \pm 1.8
MIR+Extra 1 batch	78.07 \pm 1.1	33.81 \pm 2.3	24.94 \pm 1.5
MIR+Extra 2 batches	77.10 \pm 1.4	32.36 \pm 2.8	24.65 \pm 1.5
MIR	77.50 \pm 1.6	34.42 \pm 2.4	25.21 \pm 2.2
MIR + Random Edit	77.19 \pm 1.0	35.39 \pm 3.0	24.86 \pm 0.7
MIR + Adv. Edit	78.06 \pm 1.5	35.79 \pm 0.4	25.48 \pm 1.3
MIR + GMED	79.08* \pm 0.8	36.17 \pm 2.5	26.29* \pm 1.2



(a) Split MNIST (b) Split CIFAR-10 (c) Split mini-ImgNet (d) Split MNIST (e) Split CIFAR-10 (f) Split mini-ImgNet

Figure 5: **Parameter sensitivity analysis** of the editing stride α (a,b,c) and the regularization strength β (d,e,f) for ER+GMED across various datasets. The dashed horizontal line indicates the performance of ER.

outperforms both random and adversarial edits across multiple datasets and models. This validates our choice of the editing objective.

Comparison to Increasing the Number of Replayed Examples. Recall that in MIR-GMED, we sample two independent subset of memory examples to perform editing and replay (Sec. 3.4). For a fairer comparison, we replay one (or more) extra subset of examples. Table 4 shows the performance does not improve as replaying more examples. We hypothesize that the performance is bottle-necked by the size of the memory and not the number of examples replayed.

Case study on Edited Memory Examples. In Figure 4, we show visualizations of editing of memory examples. The examples are drawn from first two task (0/1, 2/3) in the Split MNIST dataset using ER+GMED. The first and second row show the original and edited examples, noted as x_{before} and x_{after} respectively. The third row shows the difference between two $\Delta x = x_{\text{after}} - x_{\text{before}}$. While there is no significant visual differences between original and edited examples, in the difference Δx , we find examples with exaggerated contours (e.g. examples (1) and (12)) and blurring (e.g. examples (2), (3), (5), and (6)). Intuitively, ambiguous examples are exaggerated while typical examples are blurred. Our visualizations supports this intuition: examples (1) and (12) are not typically written digits, while examples (2), (3), (5), and (6) are typical. Appendix D provides a t-SNE [27] plot of the edit vector.

4.5 Analysis on the GMED Framework

Here, we analyze and ablate the various components used in the GMED framework and their effect on the final performance.

Hyper-parameter Sensitivity. In Figure 5 we plot the sensitivity of the performance of GMED with respect to two hyper-parameters: the editing stride α and the regularization strength β (Eq. 3). Clearly, ER+GMED outperforms ER over a broad range of α and β setups. Furthermore, in Figure 5 (d,e,f), better performance for non-zero β confirms the benefit of the regularization term. Recall that in our main experiments we tune the hyper-parameters α and β with only first three tasks; we note the chosen hyperparameters improve the performance despite they are not always optimal ones.

Computational Efficiency. We analyze the *additional* forward and backward computation required by ER+GMED and MIR. Compared to ER, ER+GMED adds 3 forward and 1 backward passes to estimate loss increase, and 1 backward pass to update the example. In comparison, MIR adds 3 forward and 1 backward passes with 2 of the forward passes are over a larger set of retrieval candidates. In our experiments, we found GMED has similar training time cost as MIR. In Appendix B, we report the wall-clock time, and observe the run-time of ER+GMED is 1.5 times of ER.

Increasing Steps of Editing. For experiments in Table 1, we performed one editing step over the sampled memory example x_m at time step t . In general, we can increase the number of editing steps. The direction for the edit is computed at each step, which makes the approach different from increasing the editing stride (α). Table 5 indicates that 3-step and 5-step edits in general don't

Table 5: **Editing examples for multiple gradient steps in ER+GMED.** We tune the editing stride (α) using the first three tasks as described in Sec. 3.3.

Methods / Datasets	Split MNIST	Rotated MNIST	Split CIFAR-10	Split mini-ImageNet
1-step Edit	82.21 \pm 2.9	77.50 \pm 1.6	34.84 \pm 2.2	27.27 \pm 1.8
3-step Edit	82.55 \pm 1.9	77.37 \pm 1.7	34.93 \pm 1.4	27.36 \pm 1.7
5-step Edit	83.11 \pm 1.9	77.53 \pm 1.6	36.82 \pm 1.8	26.36 \pm 2.0

lead to significant improvement in performance while incurring additional computational cost. As such, we use only 1-edit step across all our experiments.

5 Conclusion

In this paper, we propose Gradient based Memory Editing (GMED), a modular framework for memory-based task-free continual learning where examples stored in the memory can be edited. Importantly, memory examples edited by GMED are encouraged to remain in-distribution but yield increased loss in the upcoming model updates, and thus are more effective at alleviating catastrophic forgetting. We find that combining GMED with existing memory-based CL approaches leads to consistent improvements across multiple benchmark datasets, only inducing a small computation overhead. Finally, we perform a thorough ablative study to validate that the gains obtained by GMED can indeed be attributed to its editing operation and careful choice of editing objective.

Acknowledgements

This research is supported in part by the Office of the Director of National Intelligence (ODNI), Intelligence Advanced Research Projects Activity (IARPA), via Contract No. 2019-19051600007, the DARPA MCS program under Contract No. N660011924033, the Defense Advanced Research Projects Agency with award W911NF-19-20271, NSF IIS 2048211, NSF SMA 1829268, and gift awards from Google, Amazon, JP Morgan and Sony. We would like to thank all the collaborators in USC INK research lab for their constructive feedback on the work.

References

- [1] Tameem Adel, Han Zhao, and Richard E. Turner. Continual learning with adaptive weights (CLAW). In *8th International Conference on Learning Representations, ICLR 2020, Addis Ababa, Ethiopia, April 26-30, 2020*. OpenReview.net, 2020.
- [2] Rahaf Aljundi, Lucas Caccia, Eugene Belilovsky, Massimo Caccia, Min Lin, Laurent Charlin, and Tinne Tuytelaars. Online continual learning with maximally interfered retrieval. In *NeurIPS*, 2019.
- [3] Rahaf Aljundi, Klaas Kelchtermans, and Tinne Tuytelaars. Task-free continual learning. In *IEEE Conference on Computer Vision and Pattern Recognition, CVPR 2019, Long Beach, CA, USA, June 16-20, 2019*, pages 11254–11263. Computer Vision Foundation / IEEE, 2019.
- [4] Rahaf Aljundi, Min Lin, Baptiste Goujaud, and Yoshua Bengio. Gradient based sample selection for online continual learning. In Hanna M. Wallach, Hugo Larochelle, Alina Beygelzimer, Florence d’Alché-Buc, Emily B. Fox, and Roman Garnett, editors, *Advances in Neural Information Processing Systems 32: Annual Conference on Neural Information Processing Systems 2019, NeurIPS 2019, December 8-14, 2019, Vancouver, BC, Canada*, pages 11816–11825, 2019.
- [5] Pietro Buzzega, Matteo Boschini, Angelo Porrello, and Simone Calderara. Rethinking experience replay: a bag of tricks for continual learning. *ArXiv*, abs/2010.05595, 2020.
- [6] Massimo Caccia, P. Rodríguez, O. Ostapenko, Fabrice Normandin, Min Lin, L. Caccia, Issam H. Laradji, I. Rish, Alexandre Lacoste, D. Vázquez, and Laurent Charlin. Online fast adaptation and knowledge accumulation: a new approach to continual learning. *NeurIPS*, 2020.
- [7] Arslan Chaudhry, Albert Gordo, Puneet Kumar Dokania, Philip H. S. Torr, and David Lopez-Paz. Using hindsight to anchor past knowledge in continual learning. *ArXiv*, abs/2002.08165, 2020.
- [8] Arslan Chaudhry, Marc’ Aurelio Ranzato, Marcus Rohrbach, and Mohamed Elhoseiny. Efficient lifelong learning with A-GEM. In *7th International Conference on Learning Representations, ICLR 2019, New Orleans, LA, USA, May 6-9, 2019*. OpenReview.net, 2019.
- [9] Aristotelis Chrysakis and Marie-Francine Moens. Online continual learning from imbalanced data. In *Proceedings of the 37th International Conference on Machine Learning, ICML 2020, 13-18 July 2020, Virtual Event*, volume 119 of *Proceedings of Machine Learning Research*, pages 1952–1961. PMLR, 2020.
- [10] Jia Deng, Wei Dong, Richard Socher, Li-Jia Li, Kai Li, and Fei-Fei Li. Imagenet: A large-scale hierarchical image database. In *2009 IEEE Computer Society Conference on Computer Vision and Pattern Recognition (CVPR 2009), 20-25 June 2009, Miami, Florida, USA*, pages 248–255. IEEE Computer Society, 2009.

- [11] Sayna Ebrahimi, Mohamed Elhoseiny, Trevor Darrell, and Marcus Rohrbach. Uncertainty-guided continual learning with bayesian neural networks. In *8th International Conference on Learning Representations, ICLR 2020, Addis Ababa, Ethiopia, April 26-30, 2020*. OpenReview.net, 2020.
- [12] Ian J Goodfellow, Mehdi Mirza, Da Xiao, Aaron Courville, and Yoshua Bengio. An empirical investigation of catastrophic forgetting in gradient-based neural networks. *arXiv preprint arXiv:1312.6211*, 2013.
- [13] Ian J. Goodfellow, Jonathon Shlens, and Christian Szegedy. Explaining and harnessing adversarial examples. *ICLR*, 2015.
- [14] James Harrison, Apoorva Sharma, Chelsea Finn, and Marco Pavone. Continuous meta-learning without tasks. In Hugo Larochelle, Marc’Aurelio Ranzato, Raia Hadsell, Maria-Florina Balcan, and Hsuan-Tien Lin, editors, *Advances in Neural Information Processing Systems 33: Annual Conference on Neural Information Processing Systems 2020, NeurIPS 2020, December 6-12, 2020, virtual*, 2020.
- [15] Xu He, Jakub Sygnowski, Alexandre Galashov, Andrei A. Rusu, Yee Whye Teh, and Razvan Pascanu. Task agnostic continual learning via meta learning. *ArXiv*, abs/1906.05201, 2019.
- [16] Yen-Chang Hsu, Yen-Cheng Liu, Anita Ramasamy, and Zsolt Kira. Re-evaluating continual learning scenarios: A categorization and case for strong baselines. *arXiv preprint arXiv:1810.12488*, 2018.
- [17] Wenpeng Hu, Zhou Lin, Bing Liu, Chongyang Tao, Zhengwei Tao, Jinwen Ma, Dongyan Zhao, and Rui Yan. Overcoming catastrophic forgetting for continual learning via model adaptation. In *7th International Conference on Learning Representations, ICLR 2019, New Orleans, LA, USA, May 6-9, 2019*. OpenReview.net, 2019.
- [18] Khurram Javed and Martha White. Meta-learning representations for continual learning. In Hanna M. Wallach, Hugo Larochelle, Alina Beygelzimer, Florence d’Alché-Buc, Emily B. Fox, and Roman Garnett, editors, *Advances in Neural Information Processing Systems 32: Annual Conference on Neural Information Processing Systems 2019, NeurIPS 2019, December 8-14, 2019, Vancouver, BC, Canada*, pages 1818–1828, 2019.
- [19] James Kirkpatrick, Razvan Pascanu, Neil Rabinowitz, Joel Veness, Guillaume Desjardins, Andrei A Rusu, Kieran Milan, John Quan, Tiago Ramalho, Agnieszka Grabska-Barwinska, et al. Overcoming catastrophic forgetting in neural networks. *Proceedings of the national academy of sciences*, 114(13):3521–3526, 2017.
- [20] Matthias De Lange, Rahaf Aljundi, Marc Masana, Sarah Parisot, Xu Jia, A. Leonardis, Gregory Slabaugh, and T. Tuytelaars. A continual learning survey: Defying forgetting in classification tasks. *arXiv: Computer Vision and Pattern Recognition*, 2019.
- [21] Yann LeCun, Corinna Cortes, and Christopher JC Burges. The mnist database of handwritten digits, 1998. URL <http://yann.lecun.com/exdb/mnist>, 10:34, 1998.
- [22] Soochan Lee, Junsoo Ha, Dongsu Zhang, and Gunhee Kim. A neural dirichlet process mixture model for task-free continual learning. In *International Conference on Learning Representations*, 2020.
- [23] Timothée Lesort, V. Lomonaco, A. Stoian, D. Maltoni, David Filliat, and N. Rodríguez. Continual learning for robotics: Definition, framework, learning strategies, opportunities and challenges. *Inf. Fusion*, 58:52–68, 2020.
- [24] Xilai Li, Yingbo Zhou, Tianfu Wu, Richard Socher, and Caiming Xiong. Learn to grow: A continual structure learning framework for overcoming catastrophic forgetting. In Kamalika Chaudhuri and Ruslan Salakhutdinov, editors, *Proceedings of the 36th International Conference on Machine Learning, ICML 2019, 9-15 June 2019, Long Beach, California, USA*, volume 97 of *Proceedings of Machine Learning Research*, pages 3925–3934. PMLR, 2019.
- [25] B. Liu. Learning on the job: Online lifelong and continual learning. In *AAAI*, 2020.
- [26] David Lopez-Paz and Marc’Aurelio Ranzato. Gradient episodic memory for continual learning. In Isabelle Guyon, Ulrike von Luxburg, Samy Bengio, Hanna M. Wallach, Rob Fergus, S. V. N. Vishwanathan, and Roman Garnett, editors, *Advances in Neural Information Processing Systems 30: Annual Conference on Neural Information Processing Systems 2017, December 4-9, 2017, Long Beach, CA, USA*, pages 6467–6476, 2017.

- [27] Laurens van der Maaten and Geoffrey Hinton. Visualizing data using t-sne. *Journal of machine learning research*, 9(Nov):2579–2605, 2008.
- [28] Aleksander Madry, Aleksandar Makelov, Ludwig Schmidt, Dimitris Tsipras, and Adrian Vladu. Towards deep learning models resistant to adversarial attacks. In *6th International Conference on Learning Representations, ICLR 2018, Vancouver, BC, Canada, April 30 - May 3, 2018, Conference Track Proceedings*. OpenReview.net, 2018.
- [29] Jorge A Mendez and ERIC EATON. Lifelong learning of compositional structures. In *International Conference on Learning Representations*, 2021.
- [30] Cuong V. Nguyen, Yingzhen Li, Thang D. Bui, and Richard E. Turner. Variational continual learning. In *6th International Conference on Learning Representations, ICLR 2018, Vancouver, BC, Canada, April 30 - May 3, 2018, Conference Track Proceedings*. OpenReview.net, 2018.
- [31] Nicolas Papernot, P. McDaniel, Ian J. Goodfellow, S. Jha, Z. Y. Celik, and A. Swami. Practical black-box attacks against machine learning. *Proceedings of the 2017 ACM on Asia Conference on Computer and Communications Security*, 2017.
- [32] G. Parisi, Ronald Kemker, Jose L. Part, Christopher Kanan, and S. Wermter. Continual lifelong learning with neural networks: A review. *Neural networks : the official journal of the International Neural Network Society*, 113:54–71, 2019.
- [33] Anthony V. Robins. Catastrophic forgetting, rehearsal and pseudorehearsal. *Connect. Sci.*, 7:123–146, 1995.
- [34] David Rolnick, Arun Ahuja, Jonathan Schwarz, Timothy P. Lillicrap, and Gregory Wayne. Experience replay for continual learning. In Hanna M. Wallach, Hugo Larochelle, Alina Beygelzimer, Florence d’Alché-Buc, Emily B. Fox, and Roman Garnett, editors, *Advances in Neural Information Processing Systems 32: Annual Conference on Neural Information Processing Systems 2019, NeurIPS 2019, December 8-14, 2019, Vancouver, BC, Canada*, pages 348–358, 2019.
- [35] Mohammad Rostami, Soheil Kolouri, and Praveen K. Pilly. Complementary learning for overcoming catastrophic forgetting using experience replay. In Sarit Kraus, editor, *Proceedings of the Twenty-Eighth International Joint Conference on Artificial Intelligence, IJCAI 2019, Macao, China, August 10-16, 2019*, pages 3339–3345. ijcai.org, 2019.
- [36] Andrei A. Rusu, Neil C. Rabinowitz, Guillaume Desjardins, Hubert Soyer, James Kirkpatrick, Koray Kavukcuoglu, Razvan Pascanu, and Raia Hadsell. Progressive neural networks. *ArXiv*, abs/1606.04671, 2016.
- [37] Joan Serra, Didac Suris, Marius Miron, and Alexandros Karatzoglou. Overcoming catastrophic forgetting with hard attention to the task. In Jennifer G. Dy and Andreas Krause, editors, *Proceedings of the 35th International Conference on Machine Learning, ICML 2018, Stockholm, Sweden, July 10-15, 2018*, volume 80 of *Proceedings of Machine Learning Research*, pages 4555–4564. PMLR, 2018.
- [38] Hanul Shin, Jung Kwon Lee, Jaehong Kim, and Jiwon Kim. Continual learning with deep generative replay. In Isabelle Guyon, Ulrike von Luxburg, Samy Bengio, Hanna M. Wallach, Rob Fergus, S. V. N. Vishwanathan, and Roman Garnett, editors, *Advances in Neural Information Processing Systems 30: Annual Conference on Neural Information Processing Systems 2017, December 4-9, 2017, Long Beach, CA, USA*, pages 2990–2999, 2017.
- [39] Yang Song, Rui Shu, Nate Kushman, and S. Ermon. Constructing unrestricted adversarial examples with generative models. In *NeurIPS*, 2018.
- [40] Mariya Toneva, Alessandro Sordani, Remi Tachet des Combes, Adam Trischler, Yoshua Bengio, and Geoffrey J. Gordon. An empirical study of example forgetting during deep neural network learning. In *7th International Conference on Learning Representations, ICLR 2019, New Orleans, LA, USA, May 6-9, 2019*. OpenReview.net, 2019.
- [41] Gido M. van de Ven and Andreas S. Tolias. Three scenarios for continual learning. *ArXiv*, abs/1904.07734, 2019.
- [42] Oriol Vinyals, Charles Blundell, Tim Lillicrap, Koray Kavukcuoglu, and Daan Wierstra. Matching networks for one shot learning. In Daniel D. Lee, Masashi Sugiyama, Ulrike von Luxburg, Isabelle Guyon, and Roman Garnett, editors, *Advances in Neural Information Processing Systems 29: Annual Conference on Neural Information Processing Systems 2016, December 5-10, 2016, Barcelona, Spain*, pages 3630–3638, 2016.

- [43] Friedemann Zenke, Ben Poole, and Surya Ganguli. Continual learning through synaptic intelligence. In Doina Precup and Yee Whye Teh, editors, *Proceedings of the 34th International Conference on Machine Learning, ICML 2017, Sydney, NSW, Australia, 6-11 August 2017*, volume 70 of *Proceedings of Machine Learning Research*, pages 3987–3995. PMLR, 2017.
- [44] Chen Zeno, Itay Golan, E. Hoffer, and Daniel Soudry. Task agnostic continual learning using online variational bayes. *ArXiv*, abs/1803.10123, 2018.

A Implementation Details of the Compared Methods

We included detailed descriptions, and implementation details of some selected baselines in this section.

- **Experience Replay (ER)** [33, 34] stores examples in a fix-sized memory for future replay. We use reservoir sampling to decide which examples to store and replace. Following prior works [2, 3, 7], at each time step we draw the same number of examples as the batch size from the memory to replay, which are both set to 10. The algorithm is applied as is to the task-free scenario.
- **Gradient Episodic Memory (GEM)** [26] also stores examples in a memory. Before each model parameter update, GEM projects the gradient of model parameters so that the update does not incur loss increase on any previous task. The approach is however not task-free. We used a memory strength $\gamma = 0.5$ for Split MNIST and Rotated MNIST following the original work and $\gamma = 0.5$ following [4]. We applied the same γ for remaining datasets.
- **Averaged Gradient Episodic Memory (AGEM)** [8] prevents the average loss increase on a randomly drawn subset of examples from the memory. We draw $k = 256$ examples to compute the regularization at each iteration. Note that this setup of k is much larger than the number of examples drawn for replay ($k = 10$) in ER approaches. The approach is task-free.
- **Bayesian Gradient Descent (BGD)** [44] is a regularization-based continual learning algorithm. It adjusts the learning rate for parameters by estimating their certainty, noting their importance to previous data. We tune the initial standard deviation of parameters and set it as 0.011 for Split CIFAR-10 and Split CIFAR-100, 0.05 for permuted MNIST, and 0.017 for Split MNIST and Rotated MNIST. We also tune the “learning rate” hyperparameter η and set it as 8 for Split CIFAR-10 and Split CIFAR-100, and 1 for Permuted MNIST, Split MNIST, and Rotated MNIST. The approach is task-free.
- **Gradient based Sample Selection (GSS)** [4] builds upon Experience Replay (ER) by encouraging the diversity in the stored examples. We use GSS-Greedy, which is the best performing variant. The approach is task-free.
- **Hindsight Anchor Learning (HAL)** [7] learns a pseudo “anchor” example per task per class in addition to the replay memory by maximizing its estimated forgetting, and tries to fix model outputs on the anchors at training. However, unlike GMED, HAL estimates forgetting by comparing the loss before and after the model performs updates with the replay memory examples (and thus forgetting is estimated with “hindsight”). We refer to hyperparameters in the original work and set the mean embedding strength $\gamma = 0.1$, anchor learning rate as 0.001, gradient steps on anchor k as 100, and fine-tune 50 epochs on the memory to estimate forgetting across datasets. The approach is not task-free.
- **Maximally Interfering Retrieval (MIR)** [2] improves ER by selecting top forgettable examples from the memory for replay. Following the official implementation, we evaluate forgetting on a candidate set of 25 examples for mini-ImageNet dataset, and 50 examples for others. While the approach is task-free, the official implementation filter out memory examples that belong to the same task as the current data stream, which assumes knowledge about tasks boundaries. We remove this operation to adapt the method to the task-free setup. Therefore, our results are not directly comparable to the official results.
- **Neural Dirichlet Process Model for Continual Learning (CN-DPM)** [22] is a task-free model-expansion based continual learning algorithm. We report the official results in the paper. In the comparison study between ER/ER+GMED with CN-DPM, for the base model in ER/ER+GMED, we use the full expanded model in CN-DPM (*i.e.*, the model architecture when the training ends in CN-DPM). We use the same optimizer and the learning rate as CN-DPM for compared methods in this set of experiments.
- **Progressive Neural Networks (Prog. NN)** [36] is a task-aware model-expansion base approach. We treat linear layers and ResNet blocks as basic components of expansion in MLP and ResNet-18 models, *i.e.*, the model creates a new linear layer or ResNet block at each layer of the model when it encounters a new task. In addition to added components, it also introduces the connectivity between the current component and the components in previous layers as learnable parameters. The model before expansion has the same architecture and sizes as models used in other approaches such as ER.

- **Compositional Continual Learning (CompCL)** [29] is another task-aware model-expansion based approach. When the model encounters a new task, the approach performs two-stage model updates by first learning the architecture over existing and one new model component, and then performing updates on parameters of components. While the original work adds one shared component for all layers, we find it helpful to add separate components for all layers, possibly because the tasks in our setup have low similarity.

B Algorithmic and Implementation Details for GMED variants

Algorithm 2: Memory Editing with ER_{aug} (ER_{aug}+GMED)

Input: learning rate τ , edit stride α , regularization strength β , decay rate γ , model parameters θ
Receives: stream example (x_D, y_D)
Initialize: replay memory M

for $t = 1$ **to** T **do**

// draw a random mini-batch for edit and augmentation respectively
 $(x_e, y_e) \sim M$
 $k \leftarrow \text{replayed_time}(x_e, y_e)$
 $\ell_{\text{before}} \leftarrow \text{loss}(x_e, y_e, \theta_t)$
 $\ell_{\text{stream}} \leftarrow \text{loss}(x_D, y_D, \theta_t)$

//update model parameters with stream examples, discarded later
 $\theta_t' \leftarrow \text{SGD}(\ell_{\text{stream}}, \theta_t, \tau)$

//evaluate forgetting of memory examples
 $\ell_{\text{after}} \leftarrow \text{loss}(x_e, y_e, \theta_t')$
 $d \leftarrow \ell_{\text{after}} - \ell_{\text{before}}$

//edit memory examples
 $x_e' \leftarrow x_e + \gamma^k \alpha \nabla_x (d - \beta \ell_{\text{before}})$
 replace (x_e, y_e) with (x_e', y_e) in M

$(x_e^\alpha, y_e) \leftarrow \text{data_augmentation}(x_e, y_e)$
 //replay edited and augmented examples
 $\ell = \text{loss}(\{(x_e^\alpha, y_e), (x_e', y_e), (x_D, y_D)\}, \theta_t)$
 $\theta_{t+1} \leftarrow \text{SGD}(\ell, \theta_t, \tau)$
 reservoir_update(x_D, y_D, M)

end for

Algorithmic Details. We present the algorithmic details of ER_{aug}+GMED, MIR+GMED and GEM+GMED in Algorithms 2, 3 and 4. The main difference in MIR+GMED and GEM+GMED compared to ER+GMED is that we edit a separate mini-batch of memory examples from the mini-batch used for replay or regularization. Similarly, in ER_{aug}+GMED, we additionally replay a mini-batch of edited examples after data augmentation. The motivations for such design are discussed in Sec. 3.4.

Implementation Details. We implemented our models with PyTorch 1.0. We train our models with a single GTX 1080Ti or 2080Ti GPU, and we use CUDA toolkit 10.1. We use a mini-batch size of 10 throughout experiments for all approaches.

Training Time Cost. For ER+GMED, training on Split MNIST, Permuted MNIST, and Rotated MNIST takes 7 seconds, 30 seconds, and 31 seconds respectively (excluding data pre-processing). Training on Split CIFAR-10, Split CIFAR-100, and Split mini-ImageNet takes 11 minutes, 14 minutes, and 46 minutes respectively. In comparison, training with ER takes 6 seconds, 23 seconds, 16 seconds, 7 minutes, 10 minutes, and 32 minutes respectively on six datasets.

Experiment Configuration for Comparison to Model-Expansion based Methods. Model expansion based approaches such as Progressive Networks [36], Compositional Lifelong Learning [29], and CN-DPM [22] involves additional overhead by introducing new model parameters over time. We compute such overhead as the number of extra parameters when the model has fully expanded. Let n_e, n_b be the number of parameters in a fully-expanded model and a regular model in non-expansion based approaches (e.g., ER) respectively, and the difference is $\Delta n = n_e - n_b$. We report such

Algorithm 3: Memory Editing with MIR (MIR+GMED)

Input: learning rate τ , edit stride α , regularization strength β , decay rate γ , model parameters θ
Receives: stream example (x_D, y_D)
Initialize: replay memory M

for $t = 1$ **to** T **do**

- // draw a random mini-batch for edit
- $(x_e, y_e) \sim M$
- $k \leftarrow \text{replayed_time}(x_e, y_e)$
- $\ell_{\text{before}} \leftarrow \text{loss}(x_e, y_e, \theta_t)$
- $\ell_{\text{stream}} \leftarrow \text{loss}(x_D, y_D, \theta_t)$
- // retrieve a separate mini-batch of examples for replay with MIR
- $(x_m, y_m) \leftarrow \text{MIR-retrieve}(M, \theta)$
- //update model parameters with stream examples, discarded later
- $\theta'_t \leftarrow \text{SGD}(\ell_{\text{stream}}, \theta_t, \tau)$
- //evaluate forgetting of memory examples
- $\ell_{\text{after}} \leftarrow \text{loss}(x_e, y_e, \theta'_t)$
- $d \leftarrow \ell_{\text{after}} - \ell_{\text{before}}$
- //edit memory examples
- $x'_e \leftarrow x_e + \gamma^k \alpha \nabla_x (d - \beta \ell_{\text{before}})$
- replace (x_e, y_e) with (x'_e, y_e) in M
- //replay examples retrieved by MIR
- $\ell = \text{loss}(\{(x_m, y_m), (x_D, y_D)\}, \theta_t)$
- $\theta_{t+1} \leftarrow \text{SGD}(\ell, \theta_t, \tau)$
- reservoir_update(x_D, y_D, M)

end for

Algorithm 4: Memory Editing with GEM (GEM+GMED)

Input: learning rate τ , edit stride α , regularization strength β , decay rate γ , model parameters θ
Receives: stream example (x_D, y_D)
Initialize: replay memory M

for $t = 1$ **to** T **do**

- // draw a random mini-batch for edit
- $(x_e, y_e) \sim M$
- $k \leftarrow \text{replayed_time}(x_e, y_e)$
- $\ell_{\text{before}} \leftarrow \text{loss}(x_e, y_e, \theta_t)$
- $\ell_{\text{stream}} \leftarrow \text{loss}(x_D, y_D, \theta_t)$
- //update model parameters with stream examples, discarded later
- $\theta'_t \leftarrow \text{SGD}(\ell_{\text{stream}}, \theta_t, \tau)$
- //evaluate forgetting of memory examples
- $\ell_{\text{after}} \leftarrow \text{loss}(x_e, y_e, \theta'_t)$
- $d \leftarrow \ell_{\text{after}} - \ell_{\text{before}}$
- //edit memory examples
- $x'_e \leftarrow x_e + \gamma^k \alpha \nabla_x (d - \beta \ell_{\text{before}})$
- replace (x_e, y_e) with (x'_e, y_e) in M
- //Regularized model updates with GEM using the full memory
- GEM_regularized_update(x_D, y_D, M, θ)
- //Update the replay memory following GEM
- memory_update(x_D, y_D, M)

end for

overhead in the equivalent number of training examples that can be stored in a memory: given an input image with dimension (c, h, w) and the overhead Δn , the equivalent number of examples is computed as $4\Delta n/(chw + 1)$. The coefficient 4 is added because storing a model parameters in float32 type takes up 4 times as much memory as a pixel or a label y . For CN-DPM, the short-term memory used to store past examples also counts as overhead.

C Hyper-parameter Setup

Throughout experiments other than results reported in Table 2, we use SGD optimizer with a learning rate of 0.05 for MNIST datasets, 0.1 for Split CIFAR-10 and Split mini-ImageNet datasets, and 0.03 for the Split CIFAR-100 dataset across all approaches. The learning rate is tuned with ER method and fixed for all other approaches. For results reported in Table 2, we use the same optimizer and learning rates as CN-DPM. See Sec. A for setup of method specific hyperparameters.

GMED variants. Besides, GMED introduces two additional hyper-parameters: the stride of the editing α , and the regularization strength β . As we assume no access to the full data stream in the online learning setup, we cannot select hyper-parameters according to validation performance after training on the full stream. Therefore, we tune the hyper-parameters with only the validation set of first three tasks, following the practice in [8]. The tasks used for hyper-parameter search are included for computing the final accuracy, following [11]. We perform a grid search over all combinations of α and β and select the one with the best validation performance on the first three tasks. We select α from $[0.01, 0.03, 0.05, 0.07, 0.1, 0.5, 1.0, 5.0, 10.0]$, and select β from $[0, 10^{-3}, 10^{-2}, 10^{-1}, 1]$. We tune two hyper-parameters on ER+GMED and share it across MIR+GMED and GEM+GMED. We tune a separate set of hyper-parameters for ER_{aug}+GMED. Table 6 reports the optimal hyper-parameters selected for each dataset.

Table 6: Hyperparameters of the editing stride and the regularization strength selected for ER+GMED.

Dataset / Hyper-param	Editing stride α	Regularization strength β
<i>ER+GMED, MIR+GMED, GEM+GMED</i>		
Split MNIST	5.0	0.01
Permuted MNIST	0.05	0.001
Rotated MNIST	1.0	0.01
Split CIFAR-10	0.05	0.001
Split CIFAR-100	0.01	0.001
Split mini-ImageNet	1.0	0.1
<i>ER_{aug} + GMED</i>		
Split MNIST	5.0	0.001
Permuted MNIST	0.05	0.001
Rotated MNIST	1.0	0.01
Split CIFAR-10	0.07	0.01
Split CIFAR-100	0.05	0.001
Split mini-ImageNet	0.5	0.0

Sensitivity to γ . Table 7 shows the performance of GMED under various decay rates of the editing stride γ . We find $\gamma = 1.0$ (*i.e.*, no decay) consistently outperforms performance when γ is less than 1. It implies it is not necessary to explicitly discourage the deviation of edited examples from original examples with the hyper-parameter γ .

Table 7: Sensitivity of the performance of GMED to the decay rate of the editing stride (γ).

Methods / Datasets	Split MNIST	Permuted MNIST	Rotated MNIST	Split CIFAR-10	Split CIFAR-100	Split mini-ImageNet
ER	81.07 ± 2.5	78.65 ± 0.7	76.71 ± 1.6	33.30 ± 3.9	20.11 ± 1.2	25.92 ± 1.2
ER + GMED _{$\gamma=0.9$}	82.28 ± 1.7	79.07 ± 0.6	77.22 ± 1.2	33.85 ± 1.4	20.06 ± 1.8	26.92 ± 1.9
ER + GMED _{$\gamma=0.99$}	82.60 ± 2.2	79.15 ± 0.6	77.35 ± 1.3	34.10 ± 3.4	19.90 ± 1.5	27.69 ± 0.7
ER + GMED _{$\gamma=1.0$}	82.67 ± 1.9	78.86 ± 0.7	77.09 ± 1.3	34.84 ± 2.2	20.93 ± 1.6	27.27 ± 1.8
MIR	85.72 ± 1.2	79.13 ± 0.7	77.50 ± 1.6	34.42 ± 2.4	20.02 ± 1.7	25.21 ± 2.2
MIR + GMED _{$\gamma=0.9$}	85.67 ± 2.2	79.99 ± 0.7	78.45 ± 1.3	34.98 ± 0.5	19.76 ± 1.7	25.96 ± 1.2
MIR + GMED _{$\gamma=0.99$}	86.76 ± 1.2	79.76 ± 0.7	78.61 ± 0.6	35.78 ± 3.2	20.48 ± 1.7	27.70 ± 1.3
MIR + GMED _{$\gamma=1.0$}	86.52 ± 1.4	79.25 ± 0.8	79.08 ± 0.8	36.17 ± 2.5	21.22 ± 1.0	26.50 ± 1.3

D T-SNE Visualization

In Figure 6, we show the t-SNE [27] visualization of the editing vector $\Delta x = x_{\text{after}} - x_{\text{before}}$ for examples from first 2 tasks in Split MNIST. We note that the editing vectors cluster by the labels of the examples. It implies the editing performed is correlated with the labels and is clearly not random.

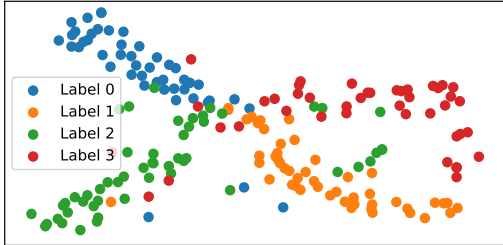


Figure 6: A t-SNE visualization of the editing performed on data examples. We use labels from the first two tasks in Split MNIST.

E Dataset Details

Following [2], we limit the number of training examples per task to 1,000 for all MNIST experiments, including Split MNIST, Permuted MNIST, and Rotated MNIST. The datasets consist of 5, 10, and 20 tasks respectively. In Split CIFAR-10, Split CIFAR-100, and Split mini-ImageNet, each task consists of 10,000, 2,500, and 2,500 training examples. For tuning hyperparameters, we separate out 5% of the training set examples in the first three tasks as the validation set. For Rotated MNIST, we limit the number of testing examples to 1,000 per task; while for other datasets, we use the complete test sets.

License and Links of Datasets. The MNIST dataset can be found in <http://yann.lecun.com/exdb/mnist/>. The dataset is released without a specific license. CIFAR-10 and CIFAR-100 can be found in <https://www.cs.toronto.edu/~kriz/cifar.html>. Similarly, the dataset is released without a license. Mini-ImageNet and its terms of use can be found in <https://mtl.yyluu.net/download/>.

Personally Identifiable Information or Offensive Content in datasets. Among all datasets we applied, MNIST is a hand-written digit classification dataset, while CIFAR and mini-ImageNet are image classification dataset over common objects. To the best of our knowledge, they do not contain any sensitive information.

F Comparison with ER+T

In addition to data augmentation over the replay memory (ER_{aug}), [5] also studied a number of other tricks, such as exponential LR decay and balanced reservoir sampling. The integrated method, referred to as ER with Tricks (ER+T), achieved SoTA performance in a task-aware, non-online setup over a number of datasets. We adapt ER+T to an online task-free continual learning setup by discarding the tricks not compatible with the online task-free scenario (namely the Bias Control (BiC) trick) and build GMED upon it. Table 8 summarizes the results. We find ER+T does not outperform ER_{aug} , *i.e.*, the tricks other than the data augmentation is not effective in a single-epoch online training setup, except Split MNIST. We further find ER+T+GMED outperforms or performs comparably with ER+T. The improvement is significant on Split MNIST and Split mini-ImageNet datasets.

Table 8: Building GMED over ER+T. * indicates significant improvement with p -value less than 0.05.

Methods / Datasets	Split MNIST	Permuted MNIST	Rotated MNIST	Split CIFAR-10	Split CIFAR-100	Split mini-ImageNet
ER + T	78.35 ± 4.5	77.71 ± 0.7	80.05 ± 1.3	47.55 ± 2.6	19.40 ± 1.5	31.25 ± 1.5
ER + T + GMED	83.02* ± 0.4	77.92 ± 0.3	79.96 ± 0.2	47.39 ± 5.0	19.75 ± 1.2	31.84* ± 1.3

Table 9: Performance of methods over data streams with fuzzy task boundaries over all six datasets. * indicates significant improvement with p -value less than 0.05.

Methods / Datasets	Split MNIST	Permuted MNIST	Rotated MNIST	Split CIFAR-10	Split CIFAR-100	Split mini-ImageNet
ER	79.74 ± 4.0	78.98 ± 0.5	76.45 ± 1.2	37.15 ± 1.6	21.99 ± 1.1	26.47 ± 2.3
ER + GMED	82.73* ± 2.6	78.91 ± 0.5	76.55 ± 1.0	40.57* ± 1.7	21.79 ± 1.9	28.20* ± 0.6
MIR	85.80 ± 1.9	79.31 ± 0.7	77.04 ± 1.2	38.70 ± 1.7	21.57 ± 1.4	25.83 ± 1.5
MIR + GMED	86.17 ± 1.7	79.26 ± 0.8	77.56* ± 1.1	41.22* ± 1.1	22.16 ± 1.1	26.86* ± 0.7
ER _{aug}	81.30 ± 2.0	77.71 ± 0.8	80.31 ± 0.9	47.97 ± 3.5	18.47 ± 2.0	31.75 ± 1.0
ER _{aug} + GMED	82.39* ± 3.7	77.68 ± 0.8	80.30 ± 1.0	51.38* ± 2.2	18.63 ± 1.3	31.83 ± 0.8

G Full Results of Experiments with Fuzzy Task Boundaries

Table 9 summarizes full results of experiments where we apply fuzzy boundaries between tasks. Experiments show that GMED generally improves performance on Split MNIST, Split CIFAR-10 and Split mini-ImageNet significantly when built upon ER, MIR, or ER_{aug}.

H Comparison to Task-Aware CL Methods

We additionally present the results of task-aware memory-based approaches in Table 10. We notice HAL was not as competitive as ER on Split MNIST, Split CIFAR-10, and Split mini-ImageNet that employs a class incremental learning setup — while in the original work, the approach was mainly test in a domain-incremental learning setup [41]. GEM performs competitively on two of the datasets (Split MNIST and Rotated MNIST), where GEM+GMED could further slightly improve the performance.

Table 10: Performance of Task-Aware Approaches.

Methods / Datasets	Split MNIST	Rotated MNIST	Split CIFAR-10	Split mini-ImageNet
HAL	77.92 ± 4.2	78.48 ± 1.5	32.06 ± 1.5	21.18 ± 2.1
GEM	87.21 ± 1.3	78.40 ± 0.5	14.81 ± 0.4	5.92 ± 0.6
GEM + GMED	87.69 ± 1.4	78.62 ± 0.4	14.13 ± 0.3	5.81 ± 0.5

I GMED without Writing Edits Back

Table 11 summarizes the result of discarding the editing performed after each time step: in these experiments, we replay the edited examples, but do not replace original examples in the memory with edited ones. The approach is noted as ER+GMED w/o writeback. We tune a separate set of editing stride and regularization strength for the method. The results indicate that ER+GMED w/o writeback achieves slightly lower performance on 5 out of 6 datasets (except Split CIFAR-10) compared to ER+GMED.

Table 11: GMED without storing back edited examples, *i.e.*, the algorithm replays edited examples, but does not update the original examples in the memory as edited ones. The results are shown after ER + GMED w/o writeback.

Methods / Datasets	Split MNIST	Permuted MNIST	Rotated MNIST	Split CIFAR-10	Split CIFAR-100	Split mini-ImageNet
ER	81.07 ± 2.5	78.85 ± 0.7	76.71 ± 1.6	33.30 ± 3.9	20.41 ± 1.2	25.92 ± 1.2
ER + GMED	82.67 ± 1.9	78.86 ± 0.7	77.09 ± 1.3	34.84 ± 2.2	20.93 ± 1.6	27.27 ± 1.8
ER + GMED w/o writeback	81.18 ± 2.6	78.49 ± 0.7	76.88 ± 1.1	34.86 ± 2.7	20.86 ± 1.6	27.20 ± 1.8

J Applying the Full Dataset in Split MNIST

In our main experiments, we sampled 1,000 training examples for Split MNIST following [3]. We further include the results of using the entire dataset for training in Table 12, and still see significant improvements.

Table 12: Performance on Split MNIST constructed from the entire MNIST training set. Note than in our main experiments, we sampled 1,000 examples per task. * and ** indicates significant improvement with $p < 0.1$ and $p < 0.01$ respectively.

Methods	w/o GMED	w/ GMED
ER	86.61 \pm 1.3	88.48** \pm 1.0
MIR	89.18 \pm 1.5	89.88** \pm 1.1
ER _{aug}	91.52 \pm 1.5	92.30* \pm 0.9

K Tabular Results of Model Performance under Various Memory Sizes

Figure 2 in the main paper present model performance under various memory size setups with bar charts. In Table 13, we further summarize results in tables, showing exact numbers of mean and standard deviation of performance. We find the improvements on Split-MNIST and Split mini-ImageNet are significant-with <0.05 over all memory size setups. Improvements on Rotated MNIST and Split CIFAR-10 are also mostly significant.

Table 13: Performance of ER, GMED+ER, MIR, and GMED+MIR with various memory sizes, shown in tables. * indicates significant improvement with $p < 0.05$.

Dataset	Split MNIST			Rotated MNIST			Split CIFAR-10		
	100	200	500	100	200	500	100	200	500
ER	71.13 \pm 1.5	77.85 \pm 1.4	81.07 \pm 2.5	63.35 \pm 1.7	70.07 \pm 1.2	76.71 \pm 1.6	21.94 \pm 1.5	26.03 \pm 2.1	33.30 \pm 3.9
ER+GMED	73.90* \pm 3.7	79.19* \pm 1.6	82.67* \pm 1.9	64.23* \pm 1.5	70.71* \pm 1.2	77.09 \pm 1.3	22.89* \pm 1.8	27.18* \pm 2.0	34.84* \pm 2.2
MIR	73.53 \pm 1.6	80.79 \pm 2.5	85.72 \pm 1.2	62.91 \pm 1.1	69.95 \pm 1.2	77.50 \pm 1.6	23.09 \pm 1.2	28.78 \pm 2.0	34.42 \pm 2.4
MIR+GMED	77.09* \pm 2.5	83.52* \pm 1.1	86.52* \pm 1.4	64.39* \pm 0.4	70.62* \pm 1.2	79.08* \pm 0.8	25.87* \pm 1.9	28.89 \pm 1.8	36.17 \pm 2.5

Dataset	Split CIFAR-100			Split mini-ImageNet		
	2000	5000	10000	5000	10000	20000
ER	12.31 \pm 1.0	16.86 \pm 0.4	20.41 \pm 1.2	18.92 \pm 0.9	25.92 \pm 1.2	29.93 \pm 1.9
ER+GMED	12.65 \pm 0.8	17.40* \pm 0.7	20.93 \pm 1.6	21.36* \pm 0.4	27.27* \pm 1.8	30.60* \pm 1.8
MIR	11.85 \pm 0.8	18.36 \pm 1.5	20.02 \pm 1.7	17.47 \pm 1.0	25.21 \pm 2.2	30.08 \pm 1.2
MIR+GMED	12.32 \pm 0.8	18.60 \pm 1.1	21.22* \pm 1.0	20.31* \pm 0.8	26.50* \pm 1.3	31.33* \pm 1.6

L Performance of Optimal Editing

Table 14 summarizes the performance of optimal editing (ER+Optimal) discussed in Sec. 4.4 compared to ER and ER+GMED. We notice that ER+Optimal outperforms ER+GMED on Split MNIST and Rotated MNIST, slightly improves on Split CIFAR-10, but does not improve on Split mini-ImageNet. The hyperparameters are not tuned extensively on mini-ImageNet because optimal editing is very expensive to compute, requiring to compute forgetting over a large sample of early examples every training step, even on moderately-sized datasets.

We hereby note that our ER+Optimal does not necessarily achieve an upper-bound performance of memory editing, as it computes optimal edit for only the coming *one* training step over the data stream. Because the edited examples may in turn affect training dynamics in future training steps, it is hard to derive an exact upper bound performance of memory editing.

M Editing Extra Examples

Table 15 summarizes the results when we edit an additional number of examples per task. We randomly sample additional examples from the memory, perform edits, and writeback, without replaying them. We notice that, over all datasets, replaying a small number of extra examples improve the performance. However, the performance drops when too many examples are edited. We hypothesize replaying additional examples per step has a similar effect to increasing the stride of

Table 14: Performance of optimal edits in Sec. 4.4 and their comparison to ER and GMED.

Methods/Datasets	Split MNIST	Rotated MNIST	Split CIFAR-10	Split mini-ImageNet
ER	80.14 \pm 3.2	76.71 \pm 1.6	33.30 \pm 3.9	25.92 \pm 1.2
ER+GMED	82.67 \pm 1.9	77.09 \pm 1.3	34.84 \pm 2.2	27.27 \pm 1.8
ER+Optimal Editing	83.40 \pm 2.6	77.73 \pm 1.3	35.04 \pm 2.6	27.01 \pm 1.6

Table 15: Results when editing an additional number of examples per step in ER+GMED.

Methods/Dataset	Split MNIST	Rotated MNIST	Split CIFAR-10	Split mini-ImageNet
ER+GMED (10 examples)	82.67±1.9	77.09±1.3	34.84±2.2	27.27±1.8
+ 3 examples	83.00±2.3	77.01±1.6	34.87±2.9	27.36±1.9
+ 5 examples	82.78±2.3	76.98±1.6	35.31±2.2	28.00±2.0
+ 10 examples	82.21±2.2	76.51±1.4	34.86±2.8	27.17±1.8
+ 50 examples	81.42±2.6	76.50±1.3	31.79±2.6	27.10±1.9

Table 16: Prediction change rate of edited examples compared to the corresponding original examples.

Dataset	Split MNIST	Rotated MNIST	Split CIFAR-10	Split mini-ImageNet
Prediction Change Rate	10.2%	2.4%	5.1%	5.5%

edits performed per example. As such, when required, the number of additional examples to edit can be an additional tunable hyperparameter in our approach.

N Prediction Change Rate of Edited Examples

We show the percentage of changed predictions after example edits in Table 16. Specifically, when the training completes, we classify examples stored in the memory (which have experienced editing) and the corresponding original examples with the model. We then compute “prediction change rate” as the portion of changed predictions over all examples stored in the memory. The prediction change implies the edited examples are more adversarial, or they can be simply artifacts to the model. However, we notice that such prediction change rate is positively correlated with performance improvement of GMED over four datasets. It implies such adversarial or artifact examples are still beneficial to reducing forgetting.

O Building Upon Other Memory Population Strategies

In all our main experiments, we used reservoir sampling to populate the replay memory. We further experiment with the greedy variant of Gradient-based Sample Selection strategy (GSS-Greedy) [4] on feasibly-sized datasets, which tries to populate the memory with more diverse examples. We report the results in Table 17. The results show GMED could still bring modest improvements when built upon GSS-Greedy.

P Ethics Statement: Societal Impact

In this work, we extend existing memory-based continual learning methods to allow gradient-based editing. We briefly discuss some of the societal impacts in this section.

Societal Impact (Positive): Improvement in Continual learning, and in particular, the online version of continual learning, can lead to potential benefits in wide variety of machine-learning tasks dealing with streaming data. With novel information being introduced by the day, it is imperative that models are not re-trained on the entire data, instead adapt and take into account the streaming data without forgoing previously learned knowledge. As an example, BERT trained on 2018 language data would be less useful for current events, but still be useful for commonsense knowledge information and as such it would be extremely beneficial if one could train over streaming current events while retaining other knowledge.

Towards this goal, a primary advantage of GMED is its integration with other memory-based continual learning frameworks. As a result, we expect advances in memory-based methods to be complemented

Table 17: Prediction change rate of edited examples compared to the corresponding original examples.

Method/Dataset	Split MNIST	Rotated MNIST
ER+GSS-Greedy	83.70±1.0	73.80±1.6
ER+GSS-Greedy+GMED	84.62±1.2	74.47±1.3
<i>p</i> -value	0.016	0.18

by GMED, incurring only a minor computational overhead – a key requirement for deploying any online continual learning algorithm in the wild.

Societal Impact (Negative): Caution must be taken in deploying our continual learning algorithms in the wild. This is because, CL algorithms at present, are validated solely on small datasets with synthetically curated streams. In the wild, the examples in the continual stream can have unexpected correlations which are not apparent in image-classification only streams.

Another key issue with continual learning is that once a knowledge is learned it is difficult to know whether it has been completely unlearned or still retained in the neural network which can be probed later. This could happen for say hospital records where patient confidentiality is needed, but were used by the continual learning model. Deleting such records is non-trivial for usual machine learning models but have dire consequences in the continual learning domain where the original stream can no longer be accessed.